博士論文

Contribution of cranial neural crest cells to cardiac development and effects of retinoic acid

(頭部神経堤細胞の心発生への寄与とレチノイン酸の効果)

瀬　谷　大　貴

Contribution of cranial neural crest cells to cardiac development and effects of retinoic acid

(頭部神経堤細胞の心発生への寄与とレチノイン酸の効果)

所属： 東京大学大学院医学系研究科

指導教員名： 栗　原　裕　基　　教授

申請者名： 瀬　谷　大　貴

Table of Contents

Abstract

The neural crest (NC), a unique multipotent stem cell population, is a hallmark of vertebrate embryonic development. Recent studies have shown that cranial NC cells (NCCs) from the preotic region, as well as cardiac (postotic) NCCs, migrate into the heart and partially differentiate into coronary artery smooth muscle cells. This dissertation aims at further characterizing the contribution of preotic NCCs to cardiac development using avian and mouse embryos as experimental models. Quail-chick chimera experiments revealed a broad distribution of preotic NCCs in the semilunar valves, right ventricular outflow region, interventricular septum and coronary arteries. NCCs contributing to the coronary artery smooth muscle layer were found to derive from the fourth rhombomere and more cranial region. Treatment of E8.5 mouse embryos with retinoic acid, a negative regulator of endothelin signaling, caused coronary artery branching abnormalities and septal branch dilatation with defective smooth muscle integrity, as observed in cranial NC ablation in chick and blockade of endothelin signaling. They were preceded by disturbed preotic NCC migration before entering the heart, which might be primarily responsible for coronary artery malformation. Finally, single-cell transcriptome analysis of NCCs in the mouse E17.5 heart revealed heterogeneity of intracardiac NCCs with two distinct subpopulations; i) Myh11- and

SM22α-positive vascular smooth muscle-like cells and ii) Sox10- and c-Kit-positive stem/progenitor-like immature cells. The present findings will serve as a basis for understanding the distinctive roles of preotic NCCs in cardiac development, function and disease processes such as in coronary artery and semilunar valve diseases.

Introduction

Neural crest and cardiovascular development

The neural crest (NC) is a multipotent stem cell population unique to vertebrates, which originates from the border between the developing neural plate and surface ectoderm[1]. NC cells (NCCs) delaminate from the dorsal neural tube through epithelial-mesenchymal transition, migrate ventrally along specific pathways and differentiate into a wide variety of cell types including neurons, glias, pigment cells and craniofacial bones and cartilages in different developmental contexts[2-4]. Disorders in the development of NC lineages cause different types of diseases. Defects in NC-derived enteric nerve development result in Hirschsprung's disease. Several types of mandibulofacial dysmorphism involving pharyngeal arch-derived structures such as Treacher-Collins syndrome are attributed to NC disorders. Some neuroectodermal tumors such as neuroblastoma, pheochromocytoma and melanoma are of NC origin. These diseases are collectively known as 'neurocristopathy', representing an entity sharing a common cellular origin although their clinical manifestations are quite different.

In cardiovascular development, the NC arising from the region between the mid-otic placode and the caudal border of somite 3, corresponding to rhombomeres (r) 6, 7 and 8,

contributes to the formation of the tunica media of pharyngeal arch (PA) artery-derived great vessels, the aorticopulmonary septum and the outflow tract endocardial cushions (Fig. 1)[5]. Ablation of the NC of this region in chick embryos results in aortic arch artery anomalies and persistent truncus arteriosus[6-8]. In addition to direct contribution to the cardiovascular structure, cardiac NCCs affect the migration and alignment of myogenic precursors derived from the second heart field contributing to outflow tract formation. The NC arising in this specific region is referred to as 'cardiac NC' since the discovery by Margaret Kirby in 1983[6]. In addition to cardiovascular components, the cardiac NC gives rise to different types of cells constituting non-cardiovascular organs such as the thymus, parathyroid glands and thyroid glands[5].

Recently, we identified cranial NCCs anterior to the otic vesicle as a novel origin of cardiac constituents[9]. These preotic NCCs originate mainly in the r4 region and are likely to share a common migratory pathway with NCCs contributing to the second PA ectomesenchyme. After migrating into the cardiac outflow tract, they distribute around the cardiac base and partly differentiate into coronary artery smooth muscle cells. In particular, the preotic NCCs contribute to the medial (smooth muscle) layer of the proximal region and septal branches, whereas the proepicardial organ-derived cells, another major origin of

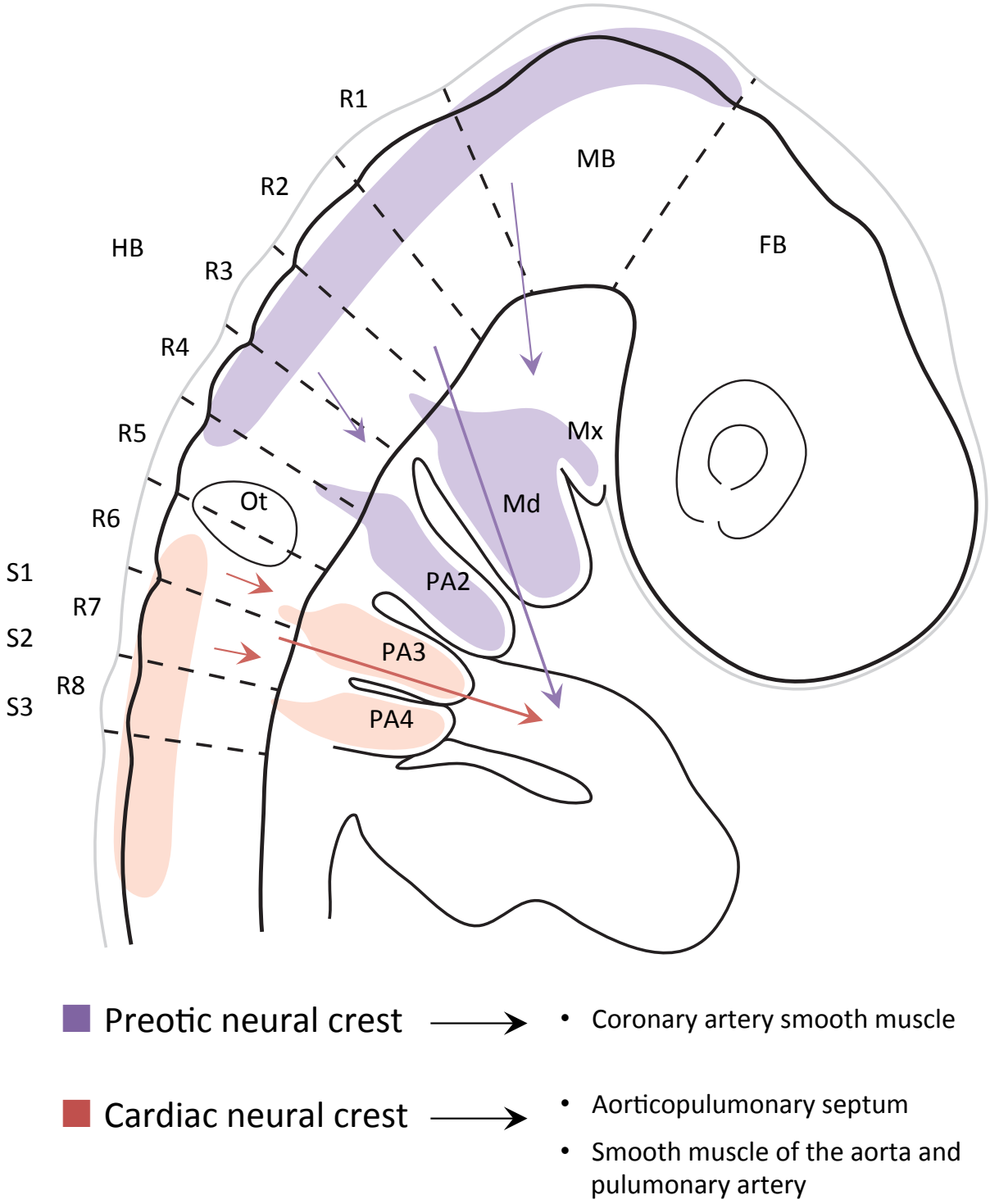

Figure 1 | Different contribution of preotic and postotic neural crest cells to cardiovascular development. FB, forebrain; HB, hindbrain; MB, midbrain; Md, mandibular arch; Mx, maxillary arch; Ot, otic vesicle; PA2-4, second to fourth pharyngeal arch; R1-8, rhombomere 1 to 8; S1-3, somite 1 to 3.

coronary artery smooth muscle cells, contribute to the distal branches[10-12]. Ablation of the preotic NC in chick embryos results in coronary artery dilatation and branching abnormalities, indicating a critical contribution of the preotic NC to normal coronary artery formation.

Neural crest and endothelin signaling

In our previous study, we also found that the endothelin (Edn) signaling is involved in preotic NC contribution to coronary artery formation[9]. Edn was originally identified as a potent vasoconstrictor and pressor peptide mainly produced by vascular endothelial cells[13]. There are three Edn isopeptides (Edn1, Edn2 and Edn3), which share two G protein-coupled receptors, Edn receptor type-A (Ednra) and type-B (Ednrb) with different affinities[14-16]. A series of previous animal and human studies have disclosed distinct roles of the Edn1/Ednra and Edn3/Ednrb pathways in the development of different NC lineages. The phenotype of mice lacking Edn1/Ednra signaling affects cranial/cardiac NC-derived structures including the craniofacial skeletons and great vessels[17-19], and is highly similar to a set of the phenotypes of the avian NC ablation model. In contrast, mice lacking Edn3/Ednrb signaling have defects in enteric neurons and melanocytes derived from trunk/vagal neural crest, resulting in megacolon and coat color spotting. Mutations in the human *EDN3* and *EDNRB*

receptor genes have been identified in patients with Hirschsprung disease. Recently, *EDNRA* mutations were identified in patients with congenital disease with mandibulofacial dysmorphism.

Mice lacking Edn1/Ednra signaling frequently demonstrated coronary artery abnormalities including branching dysmorphogenesis and septal branch dilatation, as seen in preotic NC-ablated chick embryos[9]. The absence of NC-derived smooth muscle cells in the coronary artery of *Edn1*/*Ednra*-null embryos indicates that Edn1/Ednra signaling plays an important role in the recruitment of NCCs into the coronary artery wall and subsequent smooth muscle differentiation. Correspondingly, NCC-specific deletion of $G\alpha_{12}/G\alpha_{13}$ results in similar dilatation of the coronary artery septal branch, whereas NCC-specific deletion of $G\alpha_q/G\alpha_{11}$ does not produce coronary artery abnormalities but cause craniofacial malformations similar to *Edn1*/*Ednra*-null mice[20]. These findings collectively indicate that Edn1/Ednra signaling is necessary for NCC recruitment to coronary artery formation via $G\alpha_{12}/G\alpha_{13}$ and possibly downstream Rho signaling, whereas Edn1/Ednra signaling governs the determination of the mandibular identity and morphogenesis of ventral PA structures through $G\alpha_q/G\alpha_{11}$–dependent signaling.

Retinoic acid and cardiac development

Vitamin A and its metabolic derivatives constitute a group of biologically active compounds collectively called retinoids. During vertebrate development, retinoids serve as an important morphogen that controls morphogenesis and organogenesis in various tissues and organs such as the central nervous system and limb bud[21]. In cardiovascular development, retinoid is involved in the normal process of organogenesis, and perturbations of retinoid concentration exert profound effects on it[22-24]. The involvement of retinoids in cardiogenesis was first demonstrated in vitamin A-deficient rats, which exhibited various cardiovascular abnormalities including ventricular septal defects and aortic arch anomalies[25,26]. A series of subsequent studies have revealed that a lack or excess of active (all-trans) form of retinoic acid (RA) lead to different kinds of cardiac abnormalities such as transposition of the great arteries (TGA), double outlet right ventricle (DORV) and persistent truncus arteriosus (PTA)[27,28].

Vitamin A in the diet is absorbed from the gastrointestinal tract and transported to the liver via chylomicrons. Vitamin A is then stored in the liver as retinyl esters, and is mobilized from the liver into the circulating blood as a form of retinol, normally bound to retinol-binding protein. During pregnancy, retinol in the maternal blood passes through the

placenta and is taken up from the fetal blood by target cells, where it re-binds intracellularly to cellular retinol-binding proteins. In the cytoplasm, retinol is converted to all-trans retinoic acid (RA) and via retinal by sequential enzymatic activities of the alcohol/retinol dehydrogenases and retinaldehyde dehydrogenases (Fig. 2). Retinal dehydrogenase 2 (RALDH2) is the earliest retinaldehyde dehydrogenase to be expressed, and is found in the primitive streak and mesodermal cells, and later in the somitic and lateral mesoderm, posterior heart tube and rostral forebrain[29]. Enzymes of the cytochrome P450 26 subfamily (CYP26A1, CYP26B1 and CYP26C1) catalyze reactions converting the all-trans RA into inactive metabolites[30], primarily 4-hydroxy-RA, which can be oxidized to 4-oxo-RA[31]. Alternatively, all-trans RA and its 9-cis isomer enter the nucleus and bind to retinoic acid receptors (RARα, RARβ and RARγ)[32-34] or retinoid X receptors (RXRα, RXRβ and RXRγ)[35-37], respectively. The ligand-bound receptors undergo dimerization to form RAR/RXR heterodimer[38,39] or RAR/RAR homodimer on their specific binding motifs in the chromosomal DNA known as the RA-response element (RARE), where they exert transcriptional activation or repression of the target gene.

The significance of RA signaling in cardiovascular development has been extensively dissected by the manipulation of genes coding retinoid receptors and related enzymes in mice.

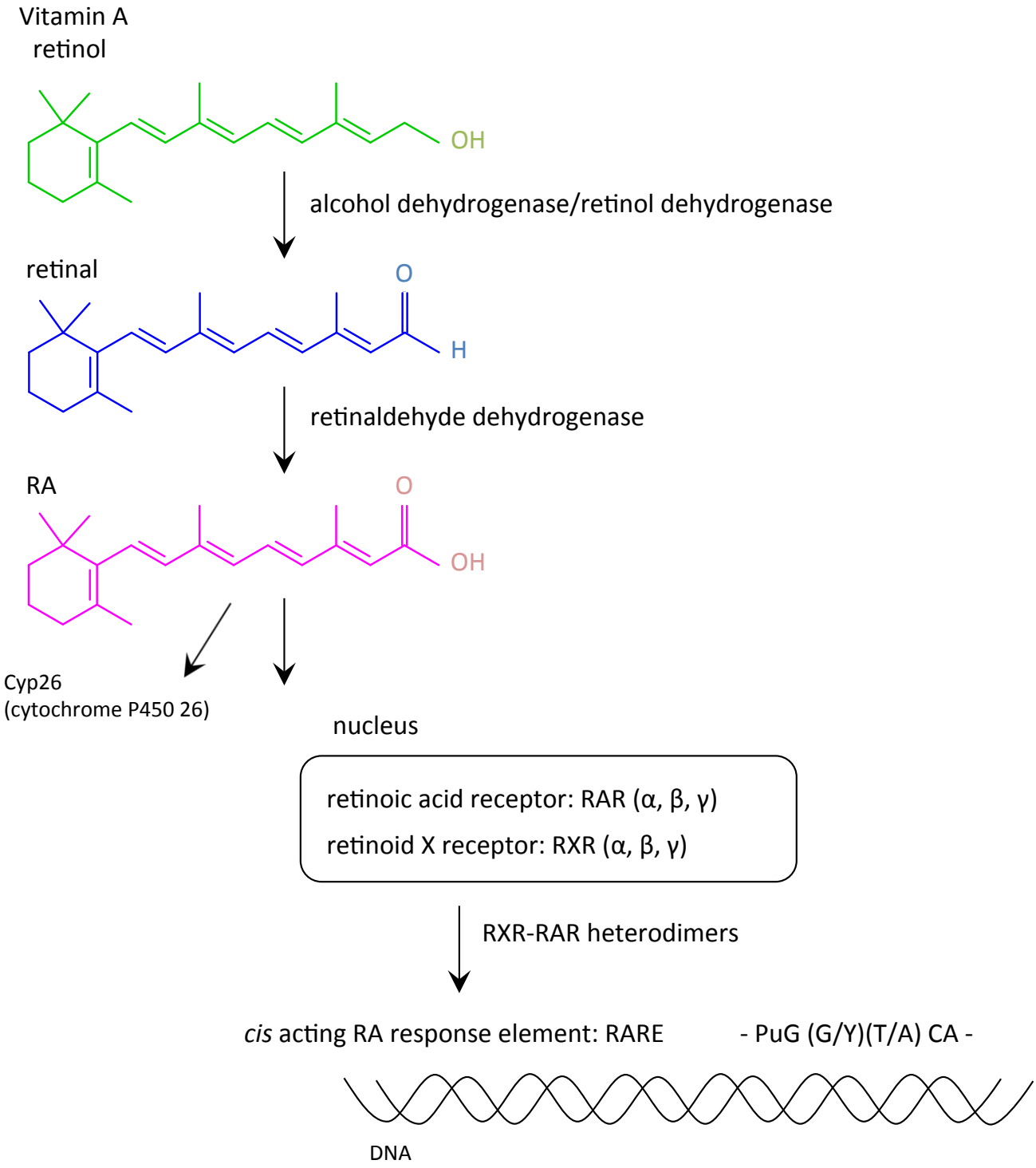

Figure 2 | Metabolic pathway and cellular mechanism of retinoic acid action.

single knockout of RXRα[40-43] and compound mutation of RAR[44-46] genes are reported to cause cardiac defects encountered in vitamin A-deficient rats, collectively indicating the importance for RXRα/RAR heterodimers in cardiac development. In contrast, exposure of embryos to excessive RA can cause different types of cardiovascular malformations dependent on developmental stages and route of RA administration[27]. These abnormalities are mostly attributed to defects in the proliferation, differentiation and migration of cardiomyocytes and their precursors.

On the other hand, aberrant RA signaling has also been shown to affect cardiovascular development through acting on NCCs. Similarity between RA-induced malformations and those associated with cardiac NC ablation has long been supposed to reflect a function of RA in the contribution of NCCs in cardiovascular development. Although recent studies indicate that the second heart field[47] and the epicardium[48] are likely to be the primary targets of RA signaling, several reports suggest the direct action of RA on NCCs. In craniofacial development, RA provokes different types of malformations by affecting the regional expression of *Edn1* and fibroblast growth factor 8 (FGF8) according to different developmental timing[49].

Purpose of this study

This disseration aims at extending our recent discovery of the contribution of the preotic (cranial) NC to coronary artery development with an involvement of Edn signaling. In particular, the following questions were addressed to make progress in understanding the roles of preotic NCCs in cardiac development, function and pathophysiology.

- Which region of the preotic NC give rise to coronary artery smooth muscle cells?
- Which components of the heart other than the coronary artery are contributed by the preotic NC?
- Can RA, a negative regulator of Edn signaling, affect the preotic NC contribution to coronary artery formation?
- If so, how can RA act on preotic NCCs?
- Which cell types are derived from the preotic NC?

Materials and Methods

Animals

The following mouse strains were used in this study: *Ednra*$^{lacZ/+}$ (*lacZ* knock-in), *Ednra*$^{EGFP/+}$ (*EGFP* knock-in)[50], *Edn1*-null (*Edn1*$^{-/-}$)[17], *Wnt1-Cre*[51], *Isl1-Cre*[52], *R26R-lacZ*[53], *R26R-eYFP*[52] mice. *Ednra*-null mice were obtained by crossing *Ednra*$^{lacZ/+}$ and/or *Ednra*$^{EGFP/+}$. *Wnt1-Cre* mice, in which Cre recombinase is expressed in precursors of neural epithelial and neural crest cells, were crossed with *R26R* reporter mice containing a *loxP*-flanked *lacZ* (or *eYFP*) cassette in the *Rosa26* locus, to generate *Wnt1-Cre;R26R* mice. In the similar manner, *Isl1-Cre;R26R* mice were used for lineage tracing of the second heart field progenitor cells. The background strains for *Ednra*$^{lacZ/+}$, *Ednra*-null, and *Edn1*-null mice were ICR, and the other mice were bred in mixed backgrounds between ICR and C57BL/6J. For timed mating, male and female mice were placed in the same cage at 9 pm, vaginal plug was detected at 1 am and mice were then separated, the midnight was considered as embryonic day (E) 0. Mice were housed in an environmentally controlled room at 21-26°C, with relative humidity of 40-60% and 12-hour light/dark cycle with allowed free access to chow and tap water. Genotypes were determined by PCR on the tail-tip or yolk sac DNA using specific primers (Table 1).

Fertilized chicken (*Gallus gallus*) and Japanese quail (*Coturnix coturnix japonica*) eggs were obtained from Shiroyama Keien Farms (Kanagawa, Japan) and Motoki Hatchery (Saitama, Japan), respectively, and were incubated in a humidified atmosphere at 37°C, until the embryos reached appropriate stages.

All animal experimentation procedures were approved by the University of Tokyo Animal Care and Use Committee and were performed in accordance with the institutional guidelines.

Retinoic Acid administration

I treated mouse embryos by gavage of mother with RA precisely at E8.5, E9.5 or E10.5 (204, 228 or 252 hours post coitum, respectively). As after oral administration RA is quickly degraded, this protocol results in exposing embryos to pharmacological levels of RA for about 2 hours[54,55]. I then analyzed the effects of this early RA exposure in embryos at E9.5 to E17.5. (Fig. 3).

A solution of all-trans RA (Sigma-Aldrich) (70 mg/mL in dimethyl sulfoxide) was diluted 1/10 in corn oil just before use and delivered by a single gavage for a final dose of 70 mg/kg of maternal body weight. Control mice received the same mixture without RA.

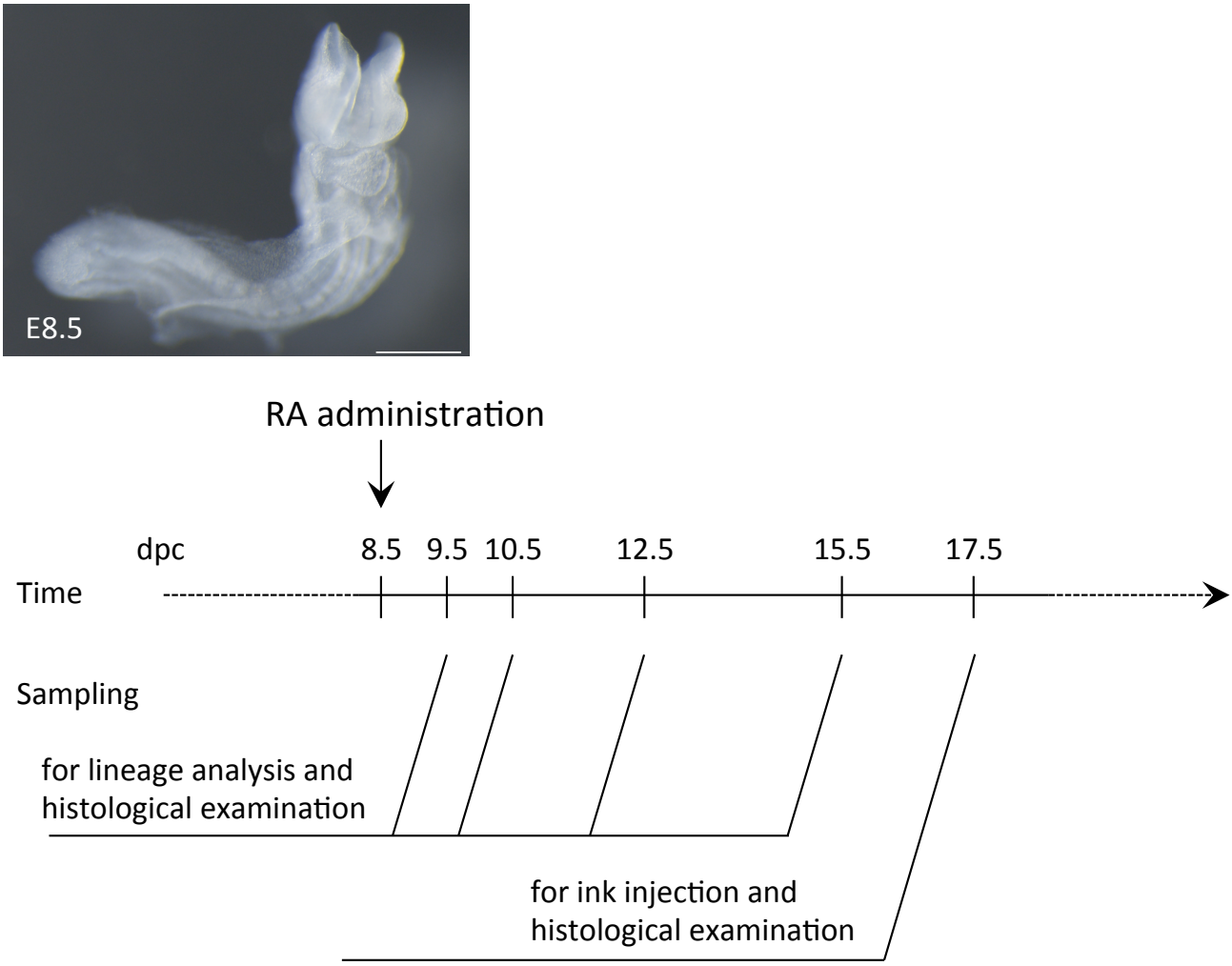

Figure 3 | All-trans retinoic acid administration and experimental schedule. dpc, day post-coitum. Scale bar, 500 μm.

Quail-chick chimera

After an incubation of the fertilized quail and chicken eggs in a humid chamber at 37°C, window was cut through the shell and embryo were visualized with India ink (Rotring, Germany) diluted 1/10 in saline solution, injected into the subgerminal cavity. In each of the transplantations, the host chicken and donor quail embryos were at comparable stages. For premigratory cranial NC (from the midbrain to the r5) and cardiac NC (from ther6-r8 and somite 4) of chimera, the 4- to 7-somite stages (ss) embryos and 6- to 9-ss embryos, respectively, were used. For control embryos the windows were opened and the somite with no treatment were counted.

Ink injection

The hearts were collected from embryos at E17.5 and dipped into heparinized phosphate-buffered saline. Then, ink (Kiwa-Guro, Sailor, Japan) was gently injected from the ascending aorta using a glass micropipette. Injected samples were fixed in 4% paraformaldehyde solution (Nacalai Tesque, Japan) and dehydrated in sequential ethanol solution. To visualize the septal branch, dehydrated samples were immersed in mixture of

benzyl alcohol and benzyl benzoate. Consecutive section was stained with haematoxylin and eosin.

Skeletal preparation

The embryos at E17.5 were fixed in 95% ethanol for one week, placed in acetone for two days at room temperature and stained with alcian blue and alizarin red[56]. Cartilage and mineralized bone were characterized by different colors (blue and red, respectively) after the stain. After washing in distilled water, the embryos were cleared with 1% potassium hydroxide and 1% potassium hydroxide in various glycerol concentrations solution until surrounding tissues turned transparent. The samples were stored in glycerol.

β-Galactosidase staining

The samples were fixed in 4% paraformaldehyde supplemented with 0.1% glutaraldehyde (Nacalai Tesque), 10 mM ethylene glycol tetraacetic acid (EGTA) and 2 mM magnesium chloride. The fixation time depends on the size of the samples. *LacZ* expression was detected by staining with X-Gal (5-bromo-4-chloro-3-indolyl β-D-galactopyranoside) for β-galactosidase activity. Whole-mount and frozen section was stained at 37°C for 4-5 hours

in the dark. For frozen sections, the samples were infiltrated in sucrose, embedded in optimal cutting temperature compound, and cryosectioned at 10 μm.

Immunohistochemistry

The samples were fixed in 4% paraformaldehyde overnight. For paraffin sections, the samples were dehydrated in ethanol, cleared in xylene, embedded in paraffin, and sectioned at 10 μm. Frozen sections were prepared in the same manner as shown above. The following primary antibodies were used in this study: mouse monoclonal anti-quail cell (QCPN, Developmental Studies Hybridoma Bank, 1/30), rabbit polyclonal anti-SM22α (Abcam, 1/1000). For chromogenic detection, I used a horseradish peroxidase-conjugated streptavidin reagent kit (VECTASTAIN, Vector Laboratories), followed by a diaminobenzidine (DAB) substrate kit (Vector Laboratories). The fluorescent stained samples were visualized with a computer-assisted confocal microscope (Nikon).

For three-dimensional reconstruction, digital image of the stained sections were processed by Amira software.

Quantitative PCR profiling of gene expression in single cells

The hearts of the *Wnt1-Cre;R26R-eYFP* embryo at E17.5 were obtained and incubated at 37°C with 0.25% trypsin-0.02% EDTA for the preparation of cell suspension. They were then suspended with culture medium (DMEM, Gibco, Life Technologies) containing 10% fetal bovine serum and filtered with 65 μm-mesh filters. The cells were then centrifuged (1000×*g*) and resuspended in DMEM. EYFP-positive cells in the suspension were collected using flow cytometer activated cell sorter, and the concentration of the cells was adjusted to 200-500 cells/μL. The sorted cells were applied to C_1 Single-Cell Auto Prep System (Fluidigm, CA, USA) and separately captured integrated fluidic circuit (IFC) plates (5-10 μm diameter, Fluidigm). Using C_1 System, cDNA library of each cell was prepared through cell lysis, reverse transcription, and preamplification by multiplex PCR using specific primers (Table 2). The cDNA library of each cell was applied to 96.96 IFC plates (Fluidigm) and quantitative PCR (qPCR) for 96 genes was performed. The qPCR data were processed by Real-time PCR Analysis software (version 4.1.2, Fluidigm), and then analyzed using Singluar Analysis Toolset (version 3.5.2, Fluidigm) on R (version 3.1.1). In the analysis, the maximal number for the detection in PCR was set at 24 cycles (Limit of Detection).

Results

Distribution of preotic neural crest cells in the developing heart revealed by quail-chick chimeras

Preotic NCCs that delaminate from the neural fold very early migrate into the heart ahead of postotic NCCs through the outflow cushion tissue[9]. To analyze the distribution of preotic NCCs after migrating into the heart, I used the quail-chick chimera technique[7,57]. In chick embryos at 4-10 ss, the neural folds spanning different regions from the forebrain to the anterior hindbrain were bilaterally excised and replaced by orthotopic quail grafts at equivalent stages (Fig. 4). Among 57 well-developed embryos after chimeric transplantation, 51 embryos showing morphologically normal heart development were subjected to further analysis. Quail-derived cells in the chimeric embryos were detected by QCPN immunostaining. Among the 51 subjects, 38 (74.5%) exhibited QCPN-positive quail cells distributing in the heart.

A detailed summary on the distribution of QCPN-positive cells after chimeric grafting is shown in Table 3. In 2 embryos which are grafted at the level of the midbrain to rhombomere (r) 2 and examined at day 4, when the aorticopulmonary septum is not yet formed, QCPN-positive cells were detected in the forming outflow cushion (Fig. 5a),

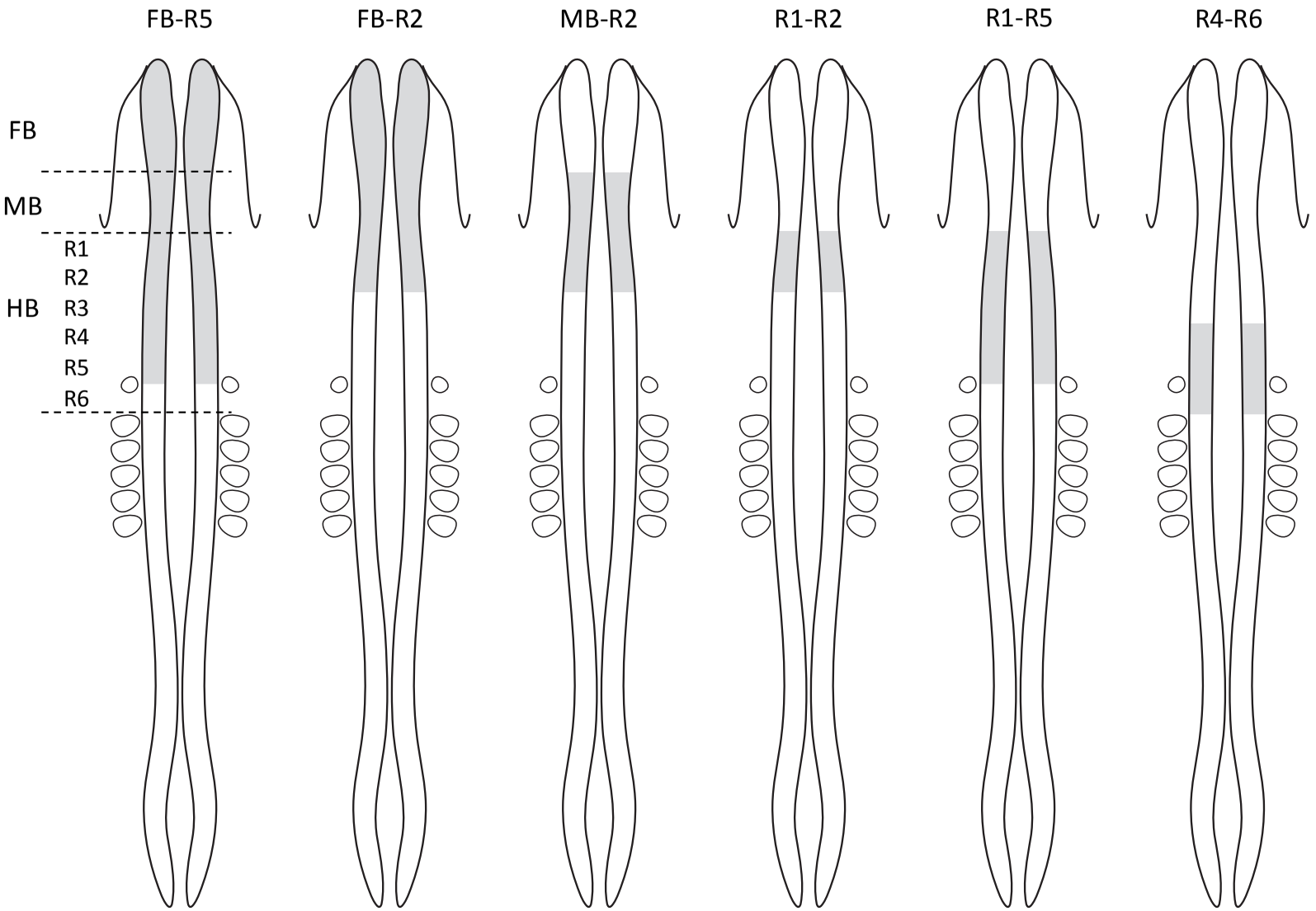

Figure 4 | Chimeric transplantation performed different regions from the forebrain to the anterior hindbrain. FB, forebrain; HB, hindbrain; MB, midbrain; R1-6, rhombomere 1 to 6.

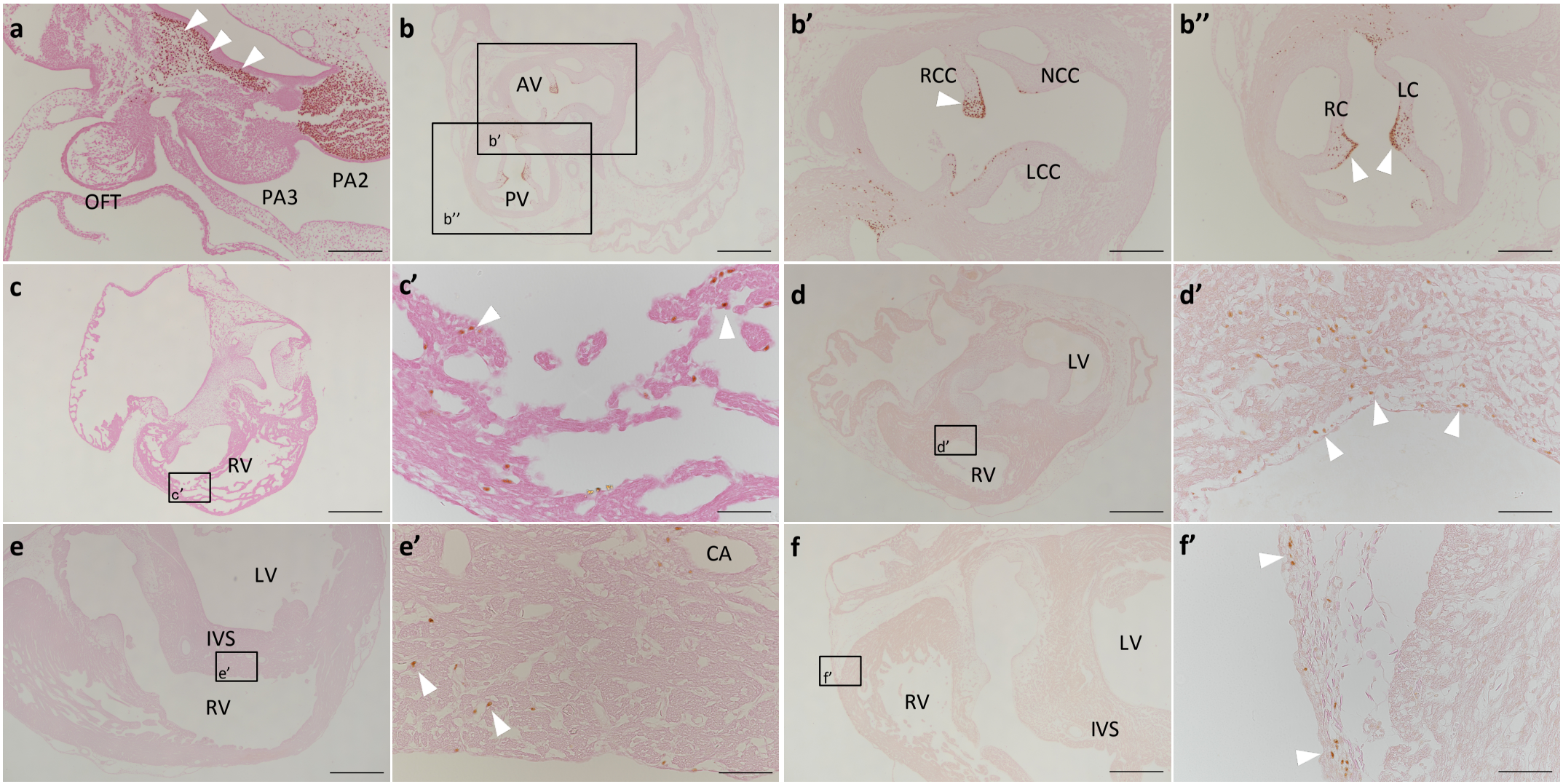

Figure 5 | Distribution of preotic neural crest cells in the heart. a-f', Immunoperoxidase method was performed with anti-QCPN to detect the quail cells. The quail preotic neural crest were detected in the outflow cushion (**a**), semilunar (aortic and pulmonary) valves (**b-b''**), right ventricular wall in the outflow region and intervenricular septum (**c-e'**), epicardial region (**f**, **f'**). White arrowheads indicate QCPN-labeled populations. AV, aortic valve; IVS, interventricular septum; CA, coronary artery; LC, left cusp; left coronary cusp; LV, left ventricle; LCC, NCC, non-coronary cusp; OFT, outflow tract; PA2-3, second to third pharyngeal arch; PV, pulmonary valve; RC, right cusp; RCC, right coronary cusp; RV, right ventricle. Scale bars, 500 μm (**b**, **c**, **d**, **e**, **f**), 200 μm (**a**, **b'**, **b''**), 50 μm (**c'**, **d'**, **e'**, **f'**).

consistent with our previous finding[27]. In embryos examined at day 8 or later, when the basic heart structures are established, QCPN-positive cells were mostly detected in the semilunar (aortic and pulmonary) valves and adjacent tissues including the aorticopulmonary septum (Fig. 5b-b''). QCPN-positive cells were also distributed in the right ventricular wall especially in the outflow region and interventricular septum (Fig. 5c-d'). In the interventricular septum, QCPN-positive cells were preferentially found near the ventricular luminal surface (Fig. 5d, d'). Contribution of QCPN-positive cells to the coronary artery was found in 10 of 36 embryos examined at day 8 or later, all of which also showed QCPN-positive cells in the right ventricle or interventricular septum (Fig. 5e, e'). Although our previous report indicates that NCCs from r4 region mainly contribute to coronary artery smooth muscle cells[9], 1 embryo grafted with the midbrain to r2 neural folds also showed QCPN-positive cells in the coronary arterial wall (Fig.6). In addition, 2 embryos grafted with the r4-r6 neural folds showed QCPN-positive cells in the tricuspid valve, although it is unclear whether the preotic (r4) or postotic (r6) NC contribute to it. QCPN-positive cells were also found in the epicardial region of 2 embryos with different grafted sites (Fig. 5f, f'). By contrast, QCPN-positive cells were not detected in the free wall of the left ventricle and the mitral valve.

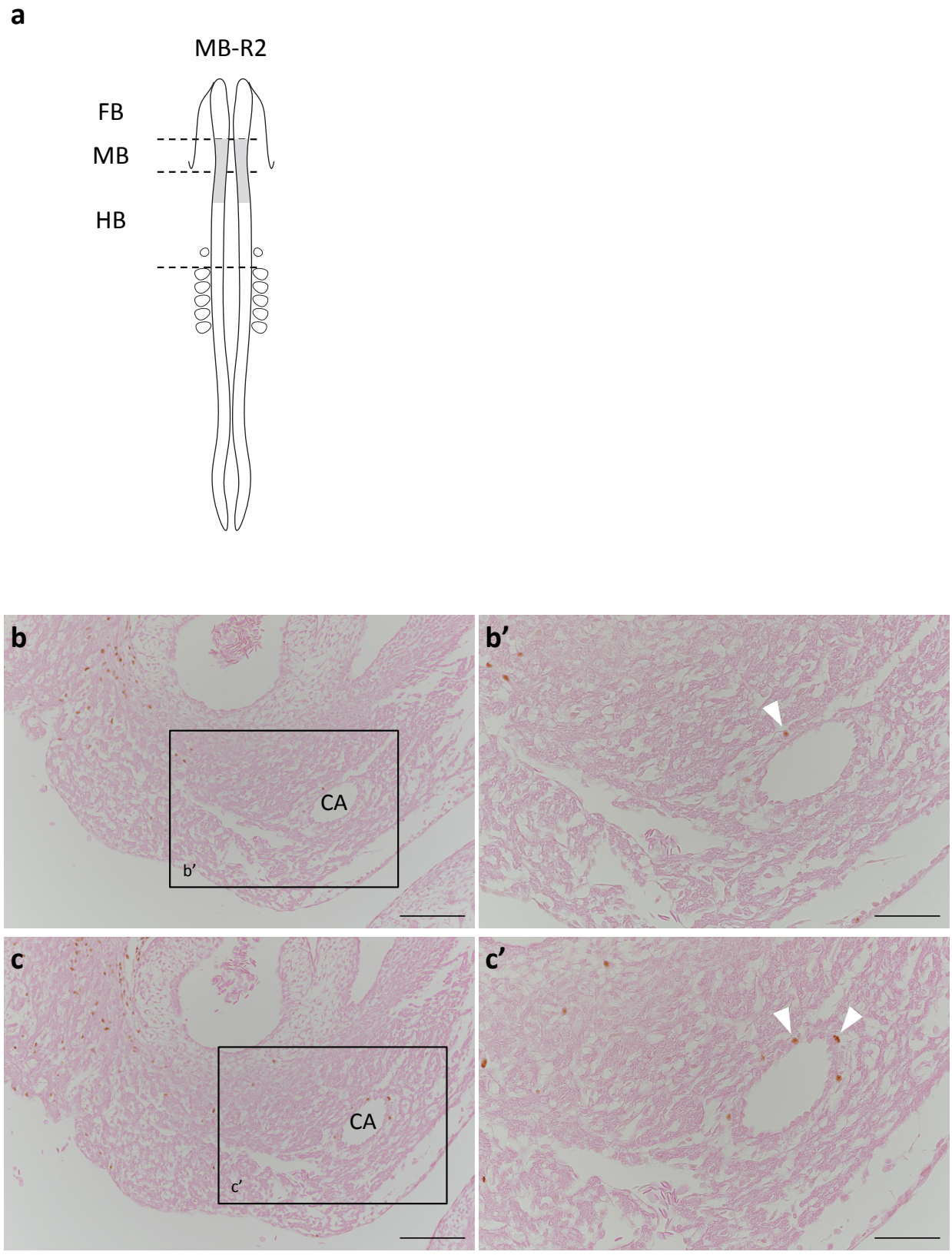

Figure 6 | Preotic neural crest cells distributed in the coronary artery. a-c', Shema of grafted preotic neural crest (**a**). Immunoperoxidase method was performed with quail cell marker antibody QCPN (**b-c'**). White arrowheads indicate QCPN-labeled populations. CA, coronary artery; FB, forebrain; HB, hindbrain; MB, midbrain; R5, rhombomere 5. Scale bars, 100 μm (**b**, **c**), 50 μm (**b'**, **c'**).

In the present analysis, I found no clear differences in regional contribution among the original neural fold levels. However, the contribution of QCPN-positive cells to the right ventricle, interventricular septum and coronary artery tends to be found in embryos undergone graft transplantation at earlier developing stages, suggesting the contribution of early migrating NCCs to these regions.

Differential distribution of preotic and postotic neural crest cells in the semilunar valves

The semilunar valves are formed from the outflow cushion following aorticopulmonary septation to divide the truncus arteriosus into the aorta and pulmonary artery*. Among three valvular leaflets for each of the aortic and pulmonary valves, the two leaflets adjacent to the aorticopulmonary septum have been shown to be abundant in NCCs, as revealed by *Wnt1-Cre* reporter mice (Fig. 7)[58]. To dissect this NCC population into different origins, I compared the distribution of preotic NCCs within the developing semilunar valvular leaflets with that of postotic NCCs. In chick embryos undergone orthotopic transplantation of quail preotic neural folds, all of the three leaflets of each semilunar valve contained QCPN-positive cells (Fig. 8). In each leaflet, QCPN-positive cells were densely located beneath the ventricular surface of the tip of the leaflet. These distribution patterns were different from

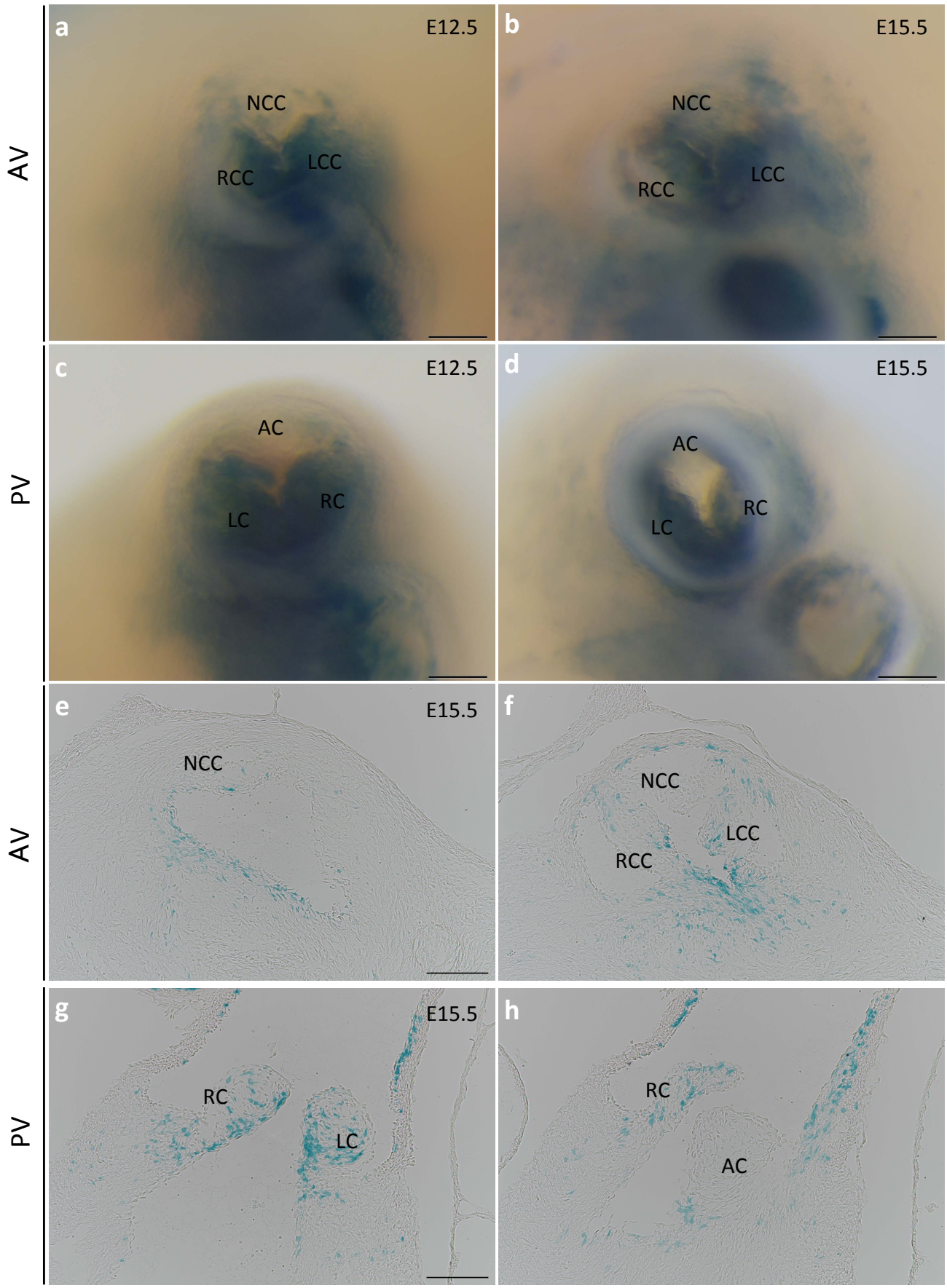

Figure 7 | Distribution of neural crest cells in semilunar valve leaflets in mice. a-g, β-galactosidase stained semilunar valve region in *Wnt1-Cre;R26R-lacZ* embryos at E12.5 (**a**, **c**) and E15.5 (**b**, **d**). β-galactosidase stained section of semilunar valve region in *Wnt1-Cre;R26R-lacZ* embryos at E15.5 (**e**, **h**). AV, aortic valve; AC, anterior cusp; LC, left cusp; LCC, left coronary cusp; NCC, non-coronary cusp; PV, pulmonary valve; RC, right cusp; RCC, right coronary cusp. Scale bars, 100 μm (**a-d**, **e**, **g**).

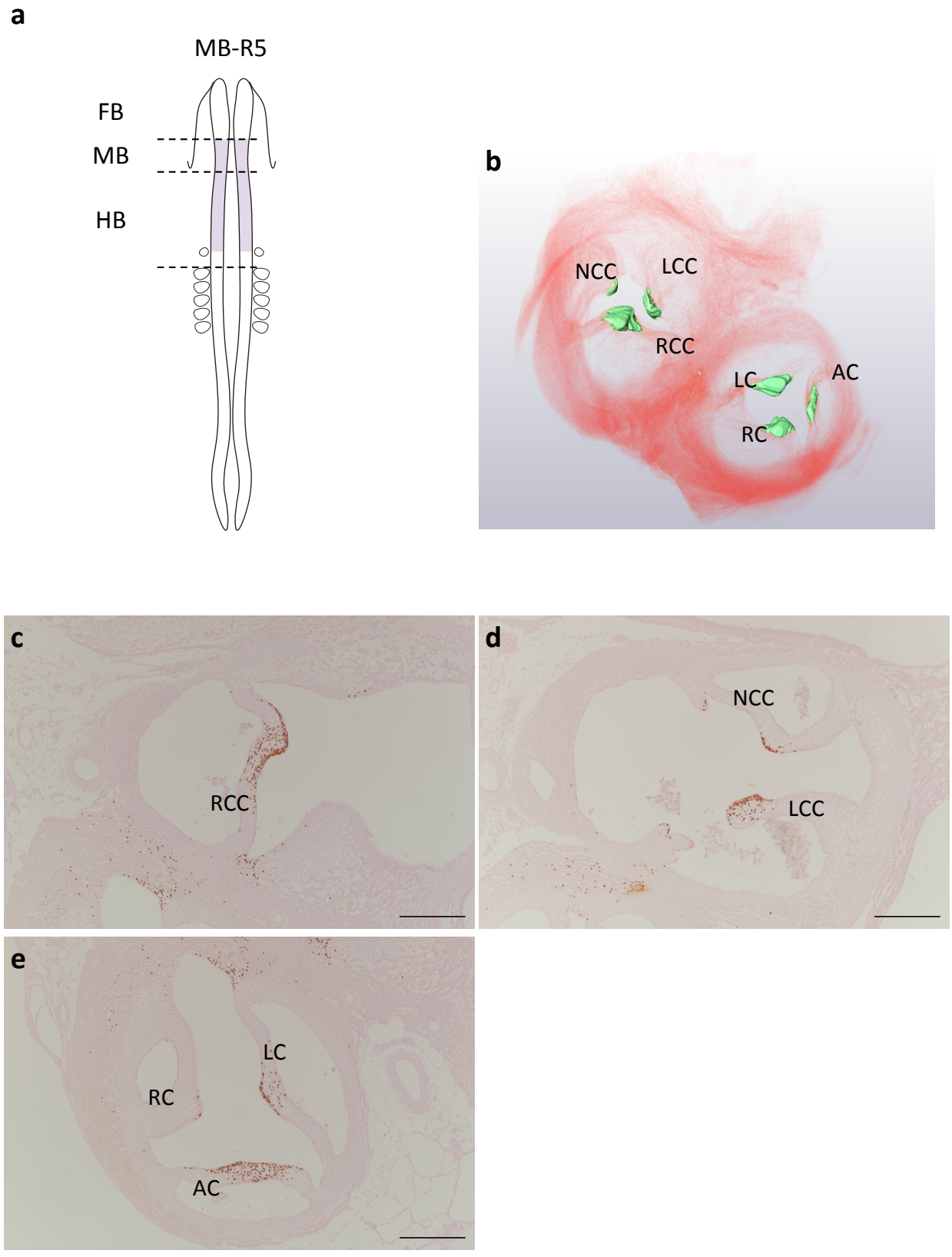

Figure 8 | Distribution of preotic neural crest cells in the semilunar valve leaflats. a-e, Shema of grafted preotic neural crest (**a**). Three-dimensional reconstruction of semilunar valves based on histological sections of quail-chick chimeric embryos (**b**). QCPN-positive cells were distributed in the three leaflets of each semilunar valve (shown in light green). Immunoperoxidase method was performed with quail cell marker antibody QCPN (**c-e**). AC, anterior cusp; CA, coronary artery; FB, forebrain; HB, hindbrain; MB, midbrain; LC, left cusp; LCC, left coronary cusp; NCC, non-coronary cusp; RC, right cusp; RCC, right coronary cusp; R5, rhombomere 5. Scale bars, 200 μm (**c-e**).

those of postotic NCCs (Fig. 9), which were detected more diffusely in the left coronary cusp of the aortic valve, with a minor distribution to the right coronary and non-coronary cusps, and three leaflets of the pulmonary valve in chick embryos undergone orthotopic transplantation of quail postotic (r6 to r8) neural folds. These results indicate that preotic and postotic NCCs contribute to semilunar valve formation in geographically different manners. The present data also suggests possible species differences in the distribution preference of NCCs in the semilunar valves between mouse and chicken, although definite conclusions should await further studies because of differences in the methodology used in the present study.

Coronary artery malformations induced by retinoic acid treatment in mouse embryos

Next, I investigated possible factors controlling the behaviors in cardiac development. Especially, I focused on RA, which has pleiotropic effects including cardiac teratogenesis. RA is also known to suppress Edn1 signaling, leading to malformation of NC-derived craniofacial structures. To explore possible effects of RA on preotic NCCs, I first focused on the morphology of the coronary arteries, which is disturbed by preotic neural crest ablation in chick embryos and inactivation of Edn1/Ednra signaling in mice[9]. To determine the critical

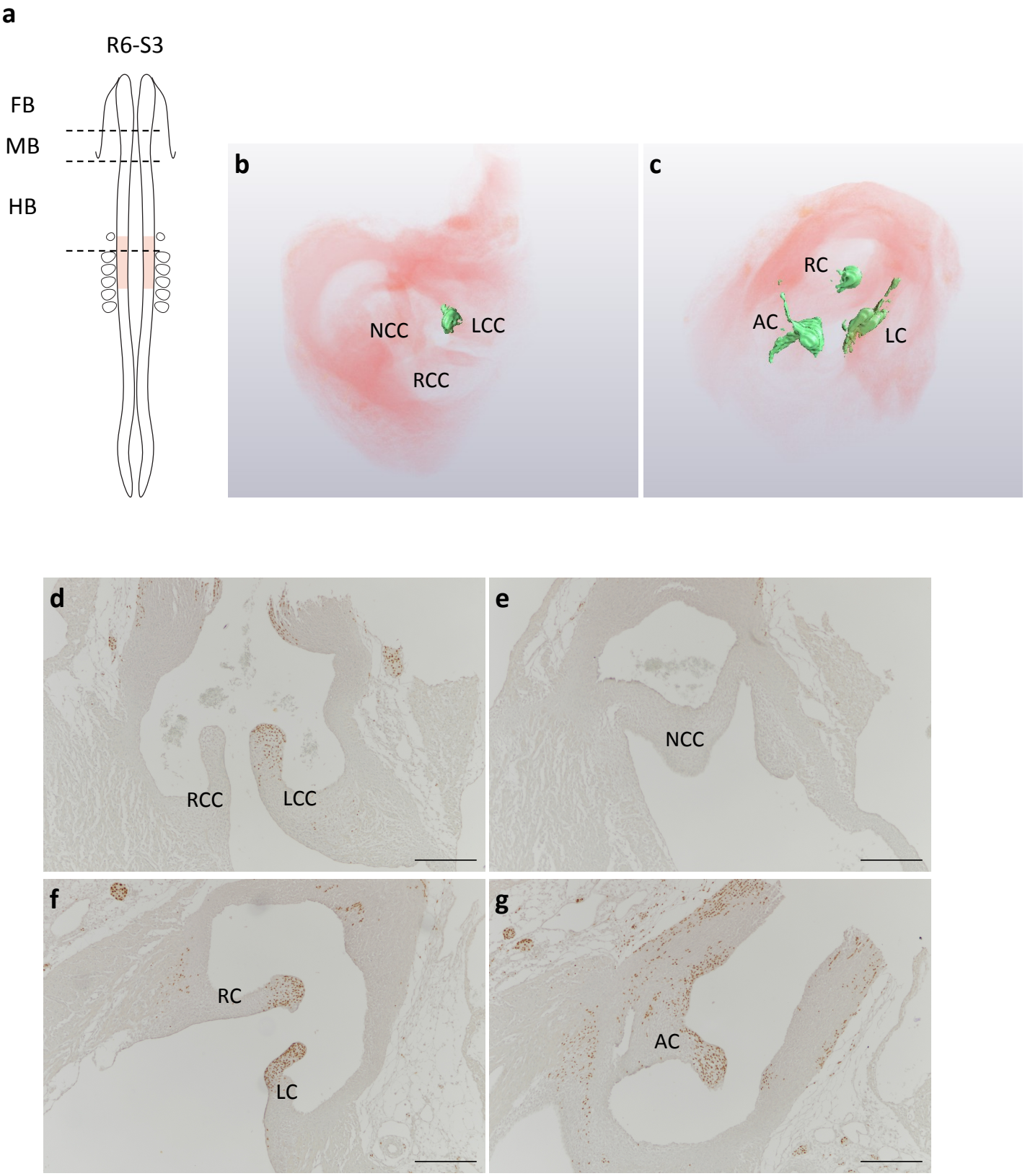

Figure 9 | Distribution of postotic neural crest cells in the semilunar valve leaflats. a-g, Shema of grafted preotic neural crest (**a**). Three-dimensional reconstruction of semilunar valves based on histological sections of quail-chick chimeric embryos (**b**, **c**). QCPN-positive cells were distributed in the left coronary cusp and three leaflets of thepulmonary valve (shown in light green). Immunoperoxidase method was performed with quail cell marker antibody QCPN (**d**-**g**). AC, anterior cusp; CA, coronary artery; FB, forebrain; HB, hindbrain; MB, midbrain; LC, left cusp; LCC, left coronary cusp; NCC, non-coronary cusp; RC, right cusp; RCC, right coronary cusp; R6, rhombomere 6; S3, somite 3. Scale bars, 200 μm (**d**-**g**).

timing of RA administration, I referred to the previous report by Vieux-Rochas et al. showing that RA provokes mandibular arch malformations at narrow optimal timing by affecting the colonization of the first pharyngeal arch by cranial (preotic) NCCs[49]. As previously reported, oral administration of RA to pregnant mice at 8.5 days post-coitum (dpc) at a dose of 70 mg/kg of maternal body weight (mg/kg bw) produced severe malformation of the mandibular arch structures represented by defects in the Meckel's cartilage and dentary bone (Fig. 10). This phenotype was similar to the transformation of the mandibular arch into maxillary-like elements in mice with inactivation of the Edn1/Ednra-Dlx5/6 pathway. Vieux-Rochas et al. speculated that RA may downregulate the Edn1/Ednra signaling to cause mandibular malformation based on the finding that Edn1 expression in the pharyngeal epithelium is decreased by RA administration. Supportively, the expression of *Ednra*, which is likely to be upregulated in *Ednra*-null mice possibly due to a lack of ligand-mediated downregulation, was increased in the first pharyngeal arch of RA-treated embryos (Fig. 11).

On the basis of these preparatory experiments, I examined the effect of RA on the formation of coronary arteries. First, I administered 70 mg/kg bw RA orally by gavage to 8.5 dpc pregnant mice and analyzed the morphology of the heart by tissue sections and coronary angiography using an ink injection technique at E17.5. Major cardiac anomalies were

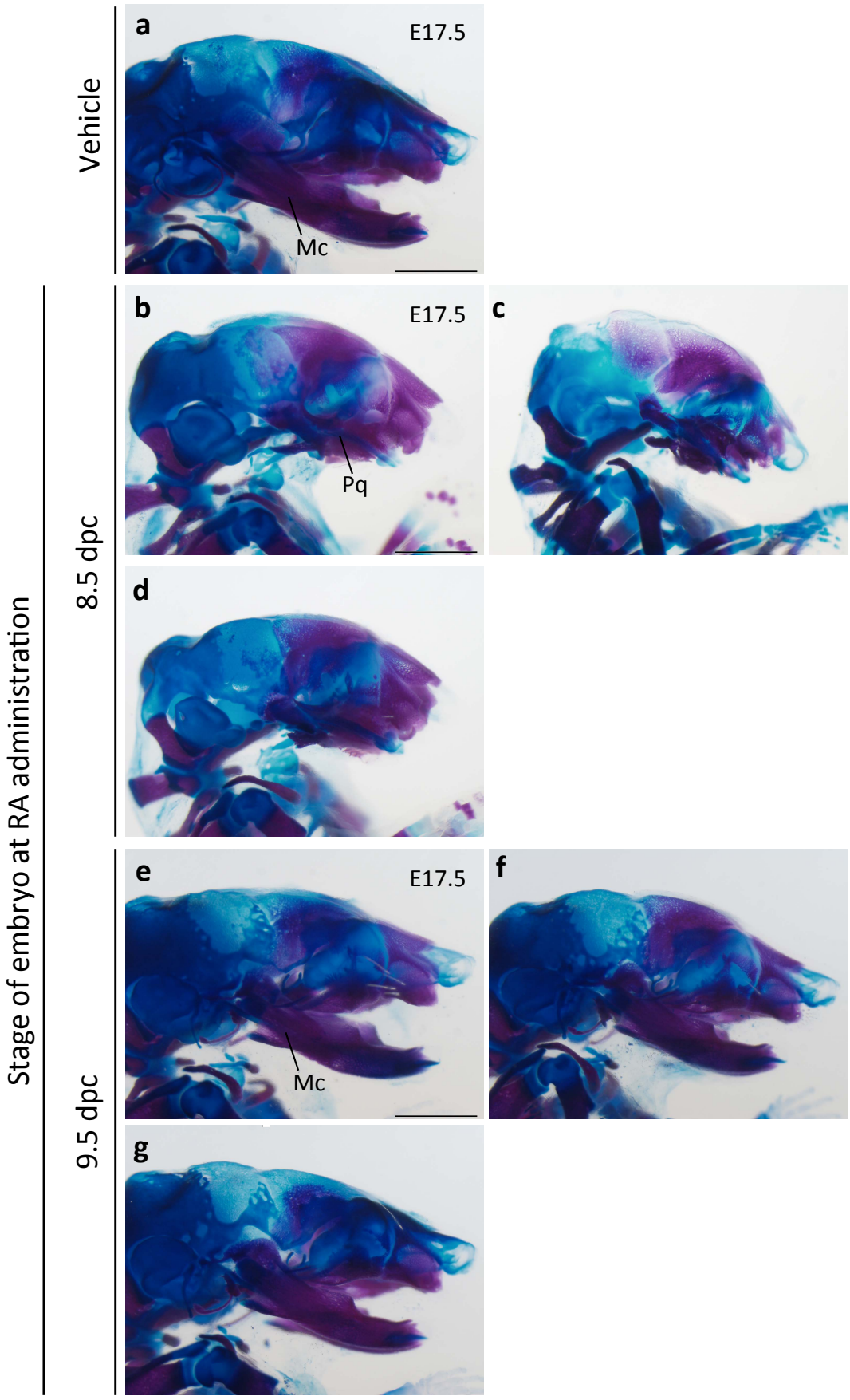

Figure 10 | Defects in the dermatocranium induced by retinoic acid treatment. a-g, Lateral view of representative dermatocrania obtained after retinoic acid administration at the indicated development al time. Homeotic-like transformation of the lower jaw into the upper jaw was reproduced by retinoic acid administration. Mc, Meckel's cartilage; Pq, palatoquadrate like bone; dpc, day post-coitum. Scale bars, 2 mm (**a**, **b**, **e**).

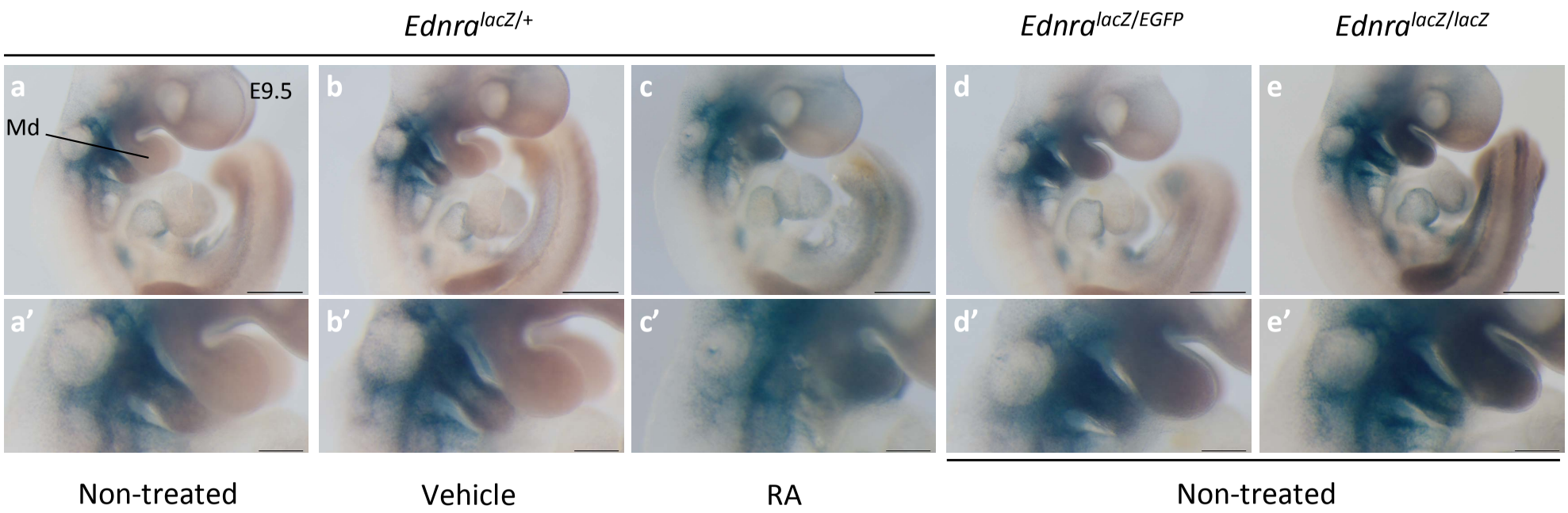

Figure 11 | Comparison of *Ednra-lacZ* expression. a-e', *Ednra*-heterozygous (**a**-**c**) and *Ednra*-homozygous (**d**, **e**) embryos stained for β-galactosidase activity. Mandibullar region is magnified in **a'**-**e'**. *Ednra* expression was extended to hinge regions of the mandibular arch in the RA-treated and *Ednra* KO embryos. Md, mandibular arch. Scale bars, 500 μm (**a**-**e**), 200 μm (**a'**-**e'**).

observed in 27 of 59 RA-treated embryos (TGA, 24/59; DORV, 3/59) (Fig. 12a-c, Table 4). Although the incidence was relatively low (7/59, 11.9%), RA treatment caused abnormal branching and luminal enlargement of the septal branch (Fig. 12f-h, 13a-c). The branching pattern and morphology of the septal branch were also affected by RA treatment. In control embryos, the septal branch initially originated from the left coronary artery before E14.5 and then reconnected to the right coronary artery, resulting in disappearance of the proximal part of the initial communication to the left coronary artery, as previously reported (Fig. 13a)[9]. In 40 of 59 RA-treated embryos (67.8%), septal branches remained originated from the left coronary artery at E17.5 (Fig 13b), as observed in *Edn1*/*Ednra*-null mice. In typical cases, the main branches of the left coronary artery were stemmed from the proximal portion of the right coronary artery (Fig. 13c). In addition, the whole contour of coronary arteries, especially in the conotruncal region, was also affected in RA-treated embryos, with dilation of the proximal portion of the left coronary artery in some case. These results suggest that the RA pathway may be critical for coronary artery formation in mice.

In histological examination, the enlarged septal branches contained red blood cells and were lined by endothelial cells. In ventricular free walls coronary arteries with apparently normal size were identified in both vehicle control and RA-treated embryos (Fig. 12f-h), as in